Solar-Terrestrial Physics. 2026, vol. 12, iss.2, pp. 69–75. DOI: 10.12737/stp-122202608. © 2026 V.V. Denisenko, S.E. Smirnov.Published by INFRA-M Academic Publishing House

DOI: 10.12737/stp-122202608
EDN: VFVTOB

Received August 26, 2025
Accepted November 07, 2025

MEASUREMENT OF THE ATMOSPHERIC ELECTRIC FIELD AT THE PARATUNKA OBSERVATORY

V.V. Denisenko
Institute of Computational Modelling SB RAS, Krasnoyarsk, Russia, denisen@icm.krasn.ru

S.E. Smirnov
Institute of Cosmophysical Research and Radio Wave Propagation FEB RAS, Paratunka, Russia, sergey@ikir.ru

Abstract. A mathematical model of the quasi-static electric field in the surface air layer in the sensor installation area is constructed with regard to its design and placement in a forest glade. The calculations are performed for the conditions of the Paratunka Geophysical Observatory. The model takes into account the influence of the contours of the glade, the height of the surrounding forest, and changes in the height of the snow cover in winter on measurements of the electric field. We calculate the calibration coefficients for the measurements, which should be used to eliminate distortions of the atmospheric electric field introduced by the measuring system.

Keywords: atmosphere, electric field, measurement, mathematical model.

INTRODUCTION

It is difficult to measure the atmospheric electric field due to the fact that the air conductivity and hence its currents are low. It is therefore necessary to develop large facilities in order to collect currents from a large area [Anisimov et al., 2014]. Although the intensity of the atmospheric electric field is hundreds and sometimes thousands of volts per meter, it cannot be measured, for example, by common voltmeters. Voltmeters have high internal resistance compared to that in electric circuits so as not to distort measured strengths, but it is not high enough to avoid distortions of electric fields in the air.

Electrostatic fluxmeters are generally used which are often referred to as “field mill” type sensors because of their design [Imyanitov, 1957]. After calibration in laboratory conditions, the sensors need additional calibration to compensate for the field distortions caused by a measuring system and other objects in the vicinity of a sensor. Nevertheless, this receives insufficient attention in studies on atmospheric electricity. Currently, there are sensors of many types, as well as a lot of ways to install them. Instrument readings vary significantly depending on the height from the Earth surface and the altitude at which observations are carried out. The GlOCAEM (GLObal Coordination of Atmospheric Electricity Measurements) database contains measurement data on surface electric fields from various points of Earth. The spread of median values of the field strength ranges from 20 to 404 V/m [Nicoll et al., 2019]. The differences are partly related to measurement methods. In this paper, the main factors distorting the field are quantified and calibration coefficients are calculated which would help eliminate these distortions.

The calculations have been carried out for the conditions of the Paratunka Geophysical Observatory. The observatory is located on the Kamchatka Peninsula near the city of Petropavlovsk-Kamchatsky, has coordinates φ=52°58′21″ N, λ=158°15′02″ E, the altitude is 76 m. The observatory employs an electrostatic fluxmeter type sensor Pole-2, developed at Voeikov Main Geophysical Observatory (St. Petersburg). To reduce measured electric field values to those on the ground, a field reduction procedure was worked out. It is described in Guidance document [Shwarts et al., 2002]. In later editions of Guidance document [Sokolenko et al., 2017], this procedure was abandoned. Some arguments in favor of such a decision and its demerits are presented in this paper.

The so-called electrode effect operates in the surface layer of the atmospheric electric field [Kupovykh et al., 1998]. The electrode effect theory deals with height distributions of positive and negative aeroions and calculates vertical profiles of air conductivity and electric field strength. Our model is based on solving the current continuity problem. With this approach, the electrode effect can be approximately taken into account only by setting altitude variations of atmospheric conductivity from results of known models. This allows us to abstract from consideration of the vertical distribution of ions of different types.

In this paper, we examine the effects of the tower, on which the sensor is installed, and the nearby forest. We also assess the role of the electrode effect that causes a decrease in air conductivity near the ground.

1. CURRENT CONTINUITY PROBLEM

We analyze only quasi-stationary measurements. Distributions of electric fields and currents in the atmosphere can therefore be found by solving the current continuity problem. A quasi-stationary model can be used to describe electric processes in the atmosphere with a typical duration exceeding 15 min [Molchanov, Hayakawa, 2008].

The basic equations for stationary electric field strength **E** and current density **j** are Faraday's law, the charge conservation law, and Ohm's law.

$$\mathrm{rot}\mathbf{E}=0, \quad (1)$$

$$\mathrm{div}\mathbf{j}=0, \quad (2)$$

$$\mathbf{j}=\sigma\mathbf{E}. \quad (3)$$

Since we deal with local phenomena and consider the conductivity to be constant, for certainty we set the value $\sigma=10^{-14}$ S/m characteristic of surface air. With constant conductivity, (2) and (3) yield $\mathrm{div}\mathbf{E}=0$, which means zero charge density in a conductor. This also applies to a moving conductor, not accounting for the negligible dynamo field. Therefore, the time of charge relaxation in the surface boundary layer does not matter for the problems we address, and the aforementioned limitation on the applicability of quasi-stationary model (1)–(3) does not appear. The exception is Section 8 in which, when assessing the role of the electrode effect, the conductivity is assumed to depend on height.

By virtue of (1), an electric potential V can be introduced such that

$$\mathbf{E}=-\mathrm{grad}V. \quad (4)$$

Then the system of equations reduces to the current continuity equation

$$-\mathrm{div}\left(\sigma\,\mathrm{grad}\,V\right)=0. \quad (5)$$

In view of (2), a vector current function **C** can be entered such that

$$\mathbf{j}=\mathrm{rot}\mathbf{C}. \quad (6)$$

We will employ it only when presenting the results. Cartesian coordinates x, y, z and the corresponding spherical coordinates r, ϑ, φ are used. For axially symmetric currents with zero azimuthal component, this vector function has only one nonzero φ component, which we denote by C. Then nonzero components of the current density

$$j_\vartheta=\frac{-1}{r}\frac{\partial\left(rC\right)}{\partial r},\ j_r=\frac{1}{r\sin\vartheta}\frac{\partial\left(C\sin\vartheta\right)}{\partial\vartheta}. \quad (7)$$

The conductivity of surface air is much lower than that of soil and seawater. The Earth surface is, therefore, usually considered as an ideal conductor. The corresponding boundary condition takes the form

$$V\big|_G=0, \quad (8)$$

where G is the boundary of the atmospheric region in question. In our models, it consists of the Earth surface and surfaces of bodies with a sufficiently high conductivity (compared to the air conductivity) so that they can be considered as ideal conductors.

We believe that there is a uniform vertical electric field in the undisturbed atmosphere. The corresponding boundary condition reads

$$V\big|_{r\to\infty}=E_0 z. \quad (9)$$

For definiteness, we assume that the given electric field has a strength E_0=260 V/m and is directed vertically downward. We have chosen this strength of the fair weather electric field over land as average from the data obtained in [Pustovalov et al., 2022]. Verticality is defined by horizontality of the Earth surface. If we set a different value of E_0, the electric fields and currents obtained below will vary proportionally. When the conductivity σ changes, only currents will vary proportionally. Therefore, all the Figures below remain valid, only the intervals between equipotentials and current lines change.

2. ANALYTICAL SOLUTION FOR THE FIELD ABOVE A HEMISPHERE

Let a perfectly conducting hemisphere with the center at the origin and radius R rise above the flat Earth surface z=0. Due to the axial symmetry and current continuity, problem (5), (8), (9) is simplified:

$$\frac{-1}{r^2}\frac{\partial}{\partial r}\left(r^2\frac{\partial V}{\partial r}\right)-\frac{1}{r^2\sin\vartheta}\frac{\partial}{\partial\vartheta}\left(\sin\vartheta\frac{\partial V}{\partial\vartheta}\right)=0, \quad (10)$$

$$V\big|_{z=0,\,r>R}=0, \quad (11)$$

$$V\big|_{r=R}=0, \quad (12)$$

$$V\big|_{r=R_\infty}=E_0 r\cos\vartheta. \quad (13)$$

The last boundary condition, unlike asymptotic condition (9), is set on a sphere of radius R_∞. This is convenient for numerical solution, so here we examine the error introduced by the finiteness of R_∞.

Resulting Dirichlet boundary value problem for Laplace equation (10)–(13) has a unique solution. It is easy to obtain its analytical solution.

$$V=\frac{E_0\cos\vartheta}{1-\left(\frac{R}{R_\infty}\right)^2}\left(r-\frac{R^2}{r}\right). \quad (14)$$

Calculate the components of the electric field strength E from Formula (4), E_φ=0,

$$E_r=\frac{-E_0\cos\vartheta}{1-\left(\frac{R}{R_\infty}\right)^2}\left(1+\frac{R^2}{r^2}\right), \quad (15)$$

$$E_\vartheta=\frac{E_0\sin\vartheta}{1-\left(\frac{R}{R_\infty}\right)^2}\left(1-\frac{R^2}{r^2}\right). \quad (16)$$

As we can see, in order for the error introduced by the finiteness of R_∞ to become less than 1 %, it is enough to take $R_\infty>10R$.

Given $R_\infty \gg R$ in view of (15, 16), the electric field above the upper point of the sphere ($r=R$, $\vartheta=0$) is vertical, directed downward, and its strength is twice as high as E_0. This means that if we could measure the field at a point at the top, we would get twice the atmospheric field. We can say that for such a measurement, according to the proposed model, a calibration coefficient K=0.5 should be used, by which sensor readings should be multiplied in order to derive the vertical component of the electric field strength in the surface air that is not distorted by such a hemisphere, i.e. for the flat Earth surface.

This doubling is maintained for any radius of a sphere. In particular, it occurs over any hummock of this shape. Formulas (15) and (16) also suggest that it is enough to rise above the hummock by ten of its radii in order for the electric field distortion, introduced by it, to become less than 1 %.

3. METHOD OF CALCULATING THE DISTORTED FIELD

Figure 1 shows a tower used to measure the surface electric field strength in Paratunka.

The sensor itself, which measures the vertical component of the field, is located in the center of the upper horizontal platform that is a circle 219 cm in radius. In the simulation, we change metal nets with a 9x9 cm cell for a solid conductor, which, apparently, can be compensated by shifting this surface a few centimeters deeper into the structure. Near the sensor, the metal surface is really solid. In order to limit ourselves to the axisymmetric model, we replace inclined aluminum beams supporting the upper platform with a circular perfectly conducting cone for which they are generating. The possibility of such a coarsening of the model will be justified later through calculations, which show that the shape of the surface lying below this platform has little effect on the field of interest above its center.

The central post of the tower is wooden, 15 cm in diameter. The conductivity of wood significantly depends on humidity and varies from 10^{-11} S/m at 20 % humidity to 10^{-6} S/m at 50 %. In Kamchatka, the air humidity is always high, and the post is dug into the ground, which further increases the humidity of its lower part we are interested in. The height of beam attachment points is only 46 cm. Even at the specified minimum humidity, the conductivity of the post $\Sigma = \pi R_w^2 \sigma_w / L \; 1.8 \cdot 10^{-13}$ S of length L=1 m. Here we use the aforementioned post radius R_w and conductivity of wood σ_w. The same is the conductivity of air column 3.4 m in radius, which is 32 times larger. At a really high humidity, the post can be considered an ideal conductor, which we do by extending condition (8) to its surface. It turned out to be a single conductor on which`

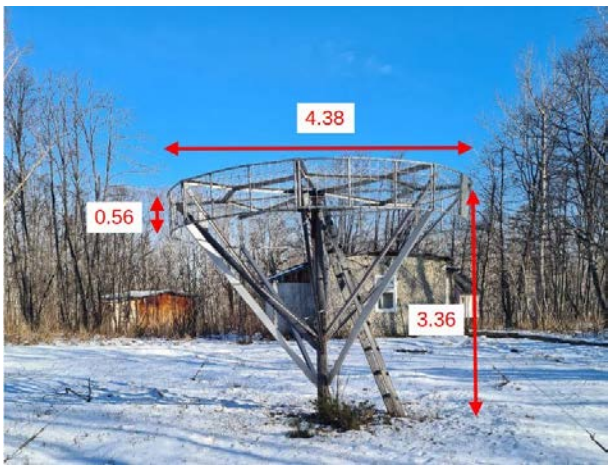

Figure 1. The tower used to measure the strength of the surface electric field in Paratunka; dimensions are in meters

zero potential is set — the ground and the entire tower.

The formulated Dirichlet boundary value problem for the Laplace equation has a unique solution. We find it numerically. Our multigrid finite-element method for the more general case of tensor conductivity problems is described in the monograph [Denisenko, 1995].

4. CALCULATION OF THE FIELD DISTORTED BY THE MEASURING TOWER

The result of the numerical solution of the problem formulated in the previous section is indicated in Figure 2 by a vertical cross-section drawn through the symmetry axis. Only a part of the calculated region is shown in which field and current distortions are noticeable. Equipotentials in 100 V increments (thick curves) and current lines (thin curves) are plotted which are cross-sections of tubes in which the current is equal to the 10 pA current multiplied by 1, 2, 3,... In other words, these are the lines of current function level C (7) in 10 pA increments. In fair weather (at a given current density of 2.6 pA/m^2), the 10 pA current flows through an air column 1.1 m in radius. Figure 2 shows this clearly: this is the radius of the first current tube.

Although we are less interested in currents, we should note that the 109 pA current is collected on the upper surface of the tower; and the 218 pA current, on the entire tower, which is 2.8 and 5.6 times more, respectively, than the 39 pA current that flows through the same column of air in the absence of the tower.

The main desired parameter is the electric field strength above the center of the upper platform of the tower, where the sensor is installed. We get 531 V/m, which is 2.04 times higher than the given field in the free atmosphere. Apparently, the field amplification due to the specific structure is close to the doubling obtained in Section 2 for the spherical tower.

To justify the possibility of replacing the set of beams supporting the platform with a solid ideally conducting cone, calculations were made for the tower with a 0.5 m decrease in the radius of this cone below the platform in the form of a horizontal step. This change in shape corresponds to the possibility for the field to penetrate

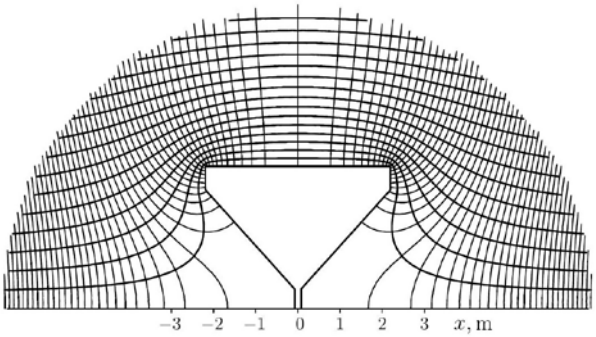

Figure 2. Distribution of electric field and currents in a vertical cross-section drawn through the symmetry axis of the measuring tower. Thick curves are equipotentials in 100 V increments; thin curves, current lines — cross-sections of tubes with a 10 pA current multiplied by 1, 2, 3…

closer to the central post beside beams. The field above the center of the tower increased by only 0.5 %,
i.e., negligibly. At the same time, the current from the atmosphere to the entire tower decreased more significantly, by 3 %, generally due to the surface below the platform. This suggests that there is a natural need for more accurate modeling when distributions of fields and currents near the bottom of the tower are of interest.

5. FIELD IN A FOREST GLADE

Consider a circular glade of radius R=14 m in a forest with trees of height H=9 m. We treat the forest as a solid conductor of thickness H, since the conductivity of fresh wood is many orders of magnitude higher than that of air, so the current flows freely through branches into the ground. At the border of the forest, we round edges of this conductor 2 m in radius. This resembles the rounding of tree crowns and allows us to avoid the meaningless feature in the solution near the corner that would be formed when representing borders of the forest area as vertical and horizontal surfaces. Thus, we have a horizontal conducting layer with a pit corresponding to the glade. The boundary of the layer depicting the forest and the ground of the glade form a single ideal conductor on which a zero potential is set. The field in the free atmosphere is given by boundary condition (9). The resulting Dirichlet boundary value problem for the Laplace equation, as in the previous section, is solved numerically.

The result of the numerical solution of this problem is presented in Figure 3 as a vertical cross-section drawn through the symmetry axis. Only a part of the calculated region is shown in which field and current distortions are noticeable. Equipotentials in 200 V increments (thick curves) and current lines (thin curves) are plotted which are cross-sections of current tubes the current in which is equal to the 200 pA current multiplied by 1, 2, 3,... In other words, these are current function lines C (7) in 200 pA increments. In fair weather (with a current density of 2.6 pA/m^2), the 200 pA current flows through an air column 5 m in radius. Figure 3 shows this clearly: the radius of the first current tube at high altitude is exactly 5 m.

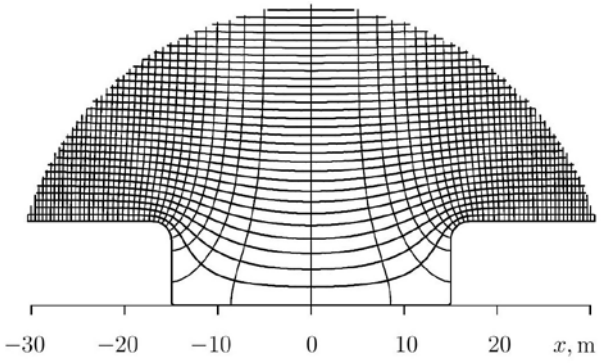

Figure 3. Distribution of electric field and currents in a vertical cross-section drawn through the symmetry axis of the glade. Thick curves are equipotentials in 200 V increments; thin curves, current lines — cross-sections of tubes in which the current is equal to the 200 pA current multiplied by 1, 2, 3, ...

Naturally, the field hardly penetrates into the pit. Near the ground in the center of the glade, the field is weakened 2.8 times compared to the field set above the forest. We can say that the calibration coefficient K=2.8 should be used for this measurement.

Thus, two main results were obtained in Sections 4 and 5.

According to this model, readings of the sensor, calibrated under ideal laboratory conditions and mounted in the measuring tower in Paratunka, should be halved if there were no forest nearby.

Judging by the results of our simulation, it would be necessary to increase 2.8 times the readings of the sensor installed in Paratunka if it were mounted on the ground in the center of a forest glade.

It could be assumed that in order to eliminate the distortions caused by both effects the sensor readings should be multiplied by 2.8/2.04=1.37. However, the glade has dimensions comparable to those of the measuring tower, so there is no reason to consider these two effects independent. Section 6 describes calculations for a geometrically more complex problem simulating the tower in the glade.

6. TOWER IN THE GLADE

Figure 4 shows the tower used to measure the surface electric field strength in Paratunka. Unlike Figure 1, the photo was taken from a quadcopter and illustrates a large area.

As we can see, the glade is not a circle centered on the axis of the tower, so the field has no axial symmetry, and current continuity problem (5), (8), (9) should be solved for a three-dimensional case. Our multigrid finite-element numerical method is described in [Denisenko, Pomozov, 2010].

Along with the tower, we consider trees, bushes, house, and snow to be good conductors adjacent to the ground. We have already mentioned that fresh

Figure 4. The tower used to measure the surface electric field strength in Paratunka; the photo was taken from a quadcopter; dimensions are in meters

wood is a good conductor, it allows the entire volume filled with branches to be treated as an ideal conductor. The characteristic conductivity of snow according to [Tentyukov et al., 2022] is 10^{-3}–10^{-2} S/m, i.e. it exceeds the conductivity of air by more than 10 orders of magnitude. We consider the forest as a continuous perfectly conducting layer 9 m high with rounded edges near its borders, which are shown in the following Figures: bushes — as a 2 m layer, at large distances there is a forest everywhere, a 6×6 m house 3 m high with a flat roof. We explore different variants with a snow cover height from 0 to 2.5 m.

Results of numerical solution of current continuity problem (5), (8), (9) in the absence of snow are presented in Figure 5. We show only the part of the calculated region, where the field disturbance is noticeable. Equipotentials are plotted in 100 V increments on a vertical plane drawn through the symmetry axis of the measuring tower in the direction of the minimum size of the glade.

On the right is the forest; on the left are bushes and forest which, along with the ground and the tower, form a perfectly conducting air boundary layer with a zero potential V=0. Figure 6 is drawn for a snow cover height S=2 m.

Figure 7 shows a typical seasonal variation in snow cover height at the Paratunka Observatory. Calculations were performed at the snow cover height from 0 to 2.5 m with a step of 0.5 m, and calibration coefficients K were found by which the sensor readings should be multiplied in order to obtain the vertical component of the electric field strength in the surface air that is not distorted by the glade and the tower, i.e. for a flat surface. The results turned out to be close to the quadratic dependence

$$K = 1.07 + 0.11\,S - 0.01\,S^2, \qquad (17)$$

the snow cover height S is given in meters. The calibration coefficient K increases from 1.07 to 1.25 with a snow cover height from 0 to 2.5 m.

7. FIELD NEAR THE GROUND IN THE GLADE

Figure 8 illustrates the distribution of the vertical component of the electric field strength near the Earth surface, related to the field in an undisturbed atmosphere, $-E_z(x, y, 0)/E_0$. The dashed circle is a projection of the measuring platform. The X-axis is shown in Figures 5 and 8, which allows us to compare field distributions in vertical (y=0 in Figure 5) and horizontal (z=0 in Figure 8) planes passing through this axis.

During additional calibration measurements at a point (–6 m, –2 m) lying near the 0.35 line (see Figure 8), the field strength was 0.34 E_1, where E_1 is the strength measured by the main sensor. The calculated value $0.35E_0$ in view of (17) corresponds to 0.38 E_1, i.e. it surprisingly accurately fits the full-scale measurement.

Note that although the calculations were carried out with an accuracy above 1 %, the initial data (the upper and lateral boundaries of the forest and bushes) is not very

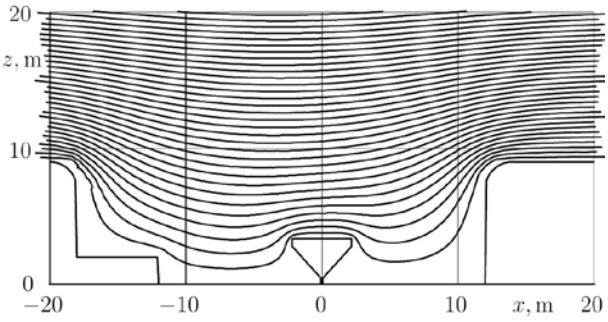

Figure 5. Electric field distribution in a vertical cross-section drawn through the symmetry axis of the measuring tower in the absence of snow. Equipotentials are plotted in 100 V increments. The lower equipotential V=0 corresponds to the air boundary layer

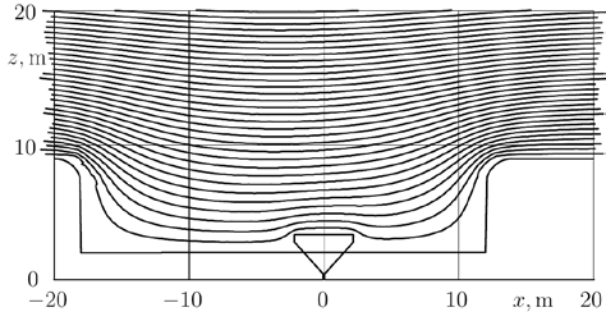

Figure 6. The same as in Figure 5 for a snow cover height S=2 m

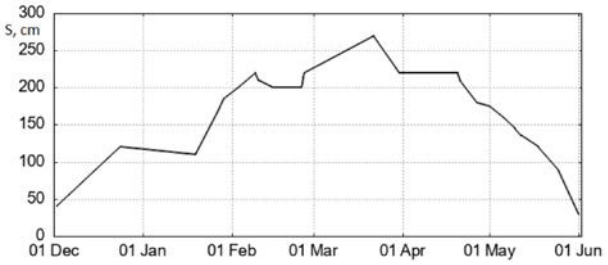

Figure 7. Variations in the snow cover height at the Paratunka Observatory in winter 2008–2009

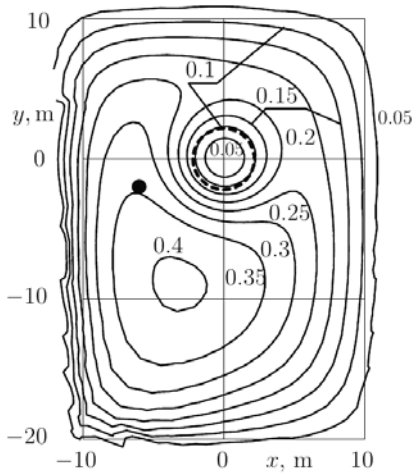

Figure 8. Ratio of the vertical component of the electric field strength near the Earth surface to the field in an undisturbed atmosphere, $-E_z(x, y, 0)/E_0$. The dashed circle is a projection of the measuring platform. The circle marks the point of additional calibration measurements (–6 m, –2 m)

accurate. For example, if the height of trees is considered to be 10 rather than 9 m, in the absence of snow we obtain K=1.3 instead of K=1.07 from (17).

8. ELECTRODE EFFECT

In reality, the constant value of atmospheric conductivity used in the previous sections is significantly distorted by the electrode effect [Morozov, 2011]. The essence of the effect is that ions carrying electric current are formed in the atmosphere, which means that when the current is directed downward near the ground there are almost no negative ions moving upward. Accordingly, the conductivity near the surface is approximately halved. In a quiescent atmosphere, the depleted layer has a meter scale. In the presence of wind due to turbu

lence, this layer thickens by an order of magnitude. In [Kupovykh et al., 1998], Figure 2.7 illustrates a typical altitude variation in the vertical component of the electric field strength E_z. It can be approximately fitted by formulas

$$\begin{aligned} -E_z(z) &= 120 - 20\left((z-20)/20\right)^2,\ z < 40, \\ -E_z(z) &= 50 + 50\exp\left(-(z-40)/25\right),\ z > 40, \end{aligned} \qquad (18)$$

where z is the height in meters; E_z, in V/m.

When the current density is constant, the conductivity is proportional to $1/E_z(z)$. Assuming the conductivity above the electrode layer equal to 10^{-14} S/m, we get $\sigma = \left(-50 / E_z(z)\right)\cdot 10^{-14}$ S/m. For ease of comparison with the results of the previous sections, we increase field strength (18) high above the ground to E_0=260 V/m (instead of 50 V/m in these formulas) and set the current density equal to 2.6 pA/m^2 (instead of 4 pA/m^2 in Figure 2.7 in [Kupovykh et al., 1998]). Recall that we have chosen the fair weather electric field strength of 260 V/m over land as an average value from the data obtained by Pustovalov et al. [2022], assuming that the results of those measurements were calibrated to represent the field outside the electrode layer. The same should be said about the normally used Carnegie data [Harrison, 2013] according to which the fair weather average field over the ocean is 130 V/m. We have already mentioned at the end of Section 2 that it is easy to change our results when these input parameters of the model are changed.

It is impossible to accurately calculate the distribution of conductivity in a turbulent electrode layer for a specific glade with the measuring tower in view of the complex processes of ionization and recombination, ion transport and transformation. Even calculating the turbulent air flow itself is problematic. Moreover, the typical process time for turbulent flow on the glade scale becomes less than a minute, which makes quasi-stationary approximation (1)–(3) inapplicable. Therefore, in this section we perform calculations only to estimate the scale of the phenomenon, assuming that current continuity model (1)–(3) is applicable with effective turbulent conductivity, whose altitude distribution we have just plotted. At the same time, we compute the height of the turbulent electrode layer from the upper boundary of the forest, and continue with a constant value down to the ground in the glade. This simplification matches the following natural assumption: in the air above the glade, the turbulence level is about the same as in the air layer located higher. Then ion concentrations and hence conductivity are about the same as in the adjacent layer tens of meters thick. If turbulence is low, the region of the electrode effect decreases to a layer about a meter thick adjacent to the ground, trees, and the tower. When analyzing Figures 5, 6, we can suppose that such a layer can be examined locally and the electric field strength near the sensor can be doubled. We do not explore this variant in detail, since, firstly, the calculation of conductivity in such a layer is complicated and, secondly, the result varies significantly depending on the wind and the turbulence level.

In the rough model of the turbulent electrode effect under study, we nevertheless reproduce the main characteristic of this effect: conductivity at the surface is approximately halved.

The results of the solution of such a problem below 10 m up to the line thickness do not differ from the potential distribution shown in Figure 5 if the interval between equipotentials is doubled. Thus, the turbulent electrode effect causes an approximate doubling of the field strength while maintaining its spatial distribution on the scale of the glade and the tower. This is not surprising because in the chosen model the conductivity is halved with precision up to 20 % below 60 m.

The electric field strength to be measured in this case is 465 V/m, i.e. 1.82 of the field above the electrode layer (E_0=260 V/m) instead of 0.93 E_0 (see Figure 5). This means a calibration coefficient K=0.55, whereas in Section 6 without regard to the electrode effect K=1.07 (17) was also obtained in the absence of snow. Thus, the measured field is approximately doubled due to the electrode effect.

We do not give an analog of Figure 8 as it, in fact, also shows only a doubling of the field compared to the field in the free atmosphere up to a few percent. This indicates that in our model the ratio between the two sensors at the top of the measuring tower and at the point on the ground, shown in Figure 8, is reproduced with high accuracy both in the presence of the turbulent electrode effect and without it. Unfortunately, this implies that it is impossible to make a reasonable conclusion about the strength of a large-scale field at heights more than a hundred meters outside the electrode layer according to the readings of such a pair of sensors installed on the measuring tower and on the ground, namely, this field is of interest in terms of the global electrical circuit (GEC). Apparently, there is a need for simultaneous calibration measurements at high altitudes, which are organized only in some geophysical observatories, for example, balloon measurements in Bork [Anisimov et al., 2023]. Note that the vertical profiles of electric field strength shown in that paper, which were obtained from balloon measurements, are much more complex than those in the simplified models on the basis of which we derived the vertical profiles of conductivity.

It may be precisely these difficulties that have led to the fact that in the latest version of Guidance document on observations of atmospheric electricity [Sokolenko et al., 2017] it is proposed to directly pre-

sent sensor data. This shifts the calibration of the measuring system from observatories onto the stage of using this data in GEC modeling, which is hardly possible without knowledge of specific measurement conditions.

CONCLUSION

The main result is Formula (17) for the calibration coefficient K. The calculations of the electric field have been carried out with high accuracy, but the initial data describing upper boundaries of the forest and bushes has not been determined very accurately. The proximity of K to 1 is not a trivial result, since the tower alone gives $K \approx 0.5$, and the round glade, considered in Section 5, separately yields $K \approx 2.8$. When processing winter measurements, it is advisable to take into account Formula (17) to obtain a correction up to 20 % due to snow.

The result of the turbulent electrode effect with the simplified model of effective conductivity is an approximate doubling of the model field strength while its spatial distribution remains unchanged on the scale of the glade and the tower. It is impossible to construct a quantitative model of this effect for specific conditions of electric field measurement.

The mathematical part of the work was financially supported by the Krasnoyarsk Mathematical Center, funded by the Ministry of Science and Higher Education of the Russian Federation as part of activities on establishment and development of regional Centers for Mathematical Research and Education (Agreement 075-02-2025-1606). The experimental part of the work was carried out under Government assignment of IKIR FEB RAS 124012300245-2.

REFERENCES

Anisimov S.V., Afinogenov K.V., Shikhova N.M. Dynamics of undisturbed midlatitude atmospheric electricity: From observations to scaling. *Radiophysics and Quantum Electronics*. 2014, vol. 56, iss. 11-12, pp. 709–722. https://doi.org/10.1007/s11141-014-9475-z.

Anisimov S.V., Aphinogenov K.V., et al. Electricity of the undisturbed atmospheric boundary layer of middle latitudes. *Izvestiya. Atmospheric and Oceanic Physics*. 2023, vol. 59, iss. 5, pp. 522–537. https://doi.org/10.1134/S000143382305002X.

Denisenko V.V. *Energy Methods for Elliptic Equations with Asymmetric Coefficients*. Novosibirsk, RAS SB Publ., 1995, 204 p. (In Russian).

Denisenko V.V., Pomozov E.V. Global electric fields in the Earth's atmosphere calculation. *J. Computational Technologies*. 2010, vol. 15, iss 5, pp. 34–50. (In Russian).

Harrison R.G. The Carnegie curve. *Surveys Geophys.* 2013, vol. 34, pp. 209–232. https://doi.org/10.1007/s10712-012-9210-2.

Imyanitov I.M. *Instruments and Methods for Studying Atmospheric Electricity*. Moscow, Gostehizdat Publ., 1957, 483 p. (In Russian).

Kupovykh G.V., Morozov V.N., Shvarts Ya.M. *Theory of the Electrode Effect in the Atmosphere*. Taganrog, Taganrog Radioteh. Univ. Publ., 1998, 122 p. (In Russian).

Molchanov O., Hayakawa M. *Seismo-Electromagnetics and Related Phenomena: History and Latest Results*. Tokyo, Terrapub, 2008, 189 p.

Morozov V.N. *Mathematical Modeling of Atmospheric-Electrical Processes Taking into Account the Influence of Aerosol Particles and Radioactive Substances*. Saint-Petersburg, Russian Gos. Hydrometeo. Univ. Publ., 2011, 253 p. (In Russian).

Nicoll K.A., Harrison R.G., et al. A global atmospheric electricity monitoring network for climate and geophysical research. *J. Atmos. Solar-Terr. Phys.* 2019, vol. 184, pp. 18–29. https://doi.org/10.1016/j.jastp.2019.01.003.

Pustovalov K., Nagorskiy P., Oglezneva M., Smirnov S. The electric field of the undisturbed atmosphere in the South of Western Siberia: A case study on Tomsk. *Atmosphere*. 2022, vol. 13, pp. 614–633. https://doi.org/10.3390/atmos13040614.

Shwarts Ya.M., Sokolenko L.G., Vychegzhanina M.E., Ryabova R.Yu. *Guidance document 52.04.168-2001: Guidelines. Observations of the Electric Field*. St. Petersburg, Hydrometeoizdat Publ., 2002, 58 p. (In Russian).

Sokolenko L.G., Popov I.B., Zainetdinov B.G. *Guidance document 52.04.168 - 2017: Observations of Atmospheric Electricity using Automated Measuring Instruments*. St. Petersburg, Hydrometeoizdat Publ., 2017, 40 p. (In Russian).

Tentyukov M., Ignatjev G., Sobolev I., Gavrilov R. Physical properties of snow cover and the mechanism of formation of geochemical barriers in snow mass. *Bull. Geosciences*. 2022, no. 5(329), pp. 26–37. (In Russian). https://doi.org/10.19110/geov.2022.5.4.

Original Russian version: Denisenko V.V., Smirnov S.E.., published in Solnechno-zemnaya fizika. 2026, vol. 12, no. 2, pp. 76–83. https://doi.org/10.12737/szf-122202608.

How to cite this article

Denisenko V.V., Smirnov S.E. Measurement of the atmospheric electric field at the Paratunka Observatory. *Sol.-Terr. Phys.* 2026, vol. 12, iss. 2, pp. 69–75. https://doi.org/10.12737/stp-122202608.